

## ADVANCED DESKTOP SEM USED FOR MEASUREMENT AND ANALYSIS OF THE ABRASIVE TOOL'S ACTIVE SURFACE

W. Kaplonek, K. Nadolny\*

Department of Production Engineering, Faculty of Mechanical Engineering, Koszalin University of Technology, Koszalin, Poland.

\*Corresponding author, e-mail: krzysztof.nadolny@tu.koszalin.pl, phone: +48 94 3478412.

Recibido: Enero 2013. Aprobado: Mayo 2013.

Publicado: Mayo 2013.

### ABSTRACT

The need to carry out broader and more thorough research using scanning electron microscopes gives birth to the need for developing a new class of low-cost, small-sized instruments with plenty of measurement capabilities. A new technical solution in this respect are advanced desktop SEMs, characterized by a number of metrological parameter advantages. This work is focused on presenting recent solutions in the field of electron microscopy as potentially new and effective measurement techniques that may be widely used in various fields of modern science and technology. The Authors analyzed the possibility of using modern desktop SEM Phenom G2 Pro by Phenom-World for observation and analysis of abrasive tools' surfaces. A number of small-sized grinding wheels with ceramic bond were used in the experimental tests. The condition of the active surfaces of these grinding wheels was thoroughly analyzed using the dedicated Phenom™ Pro Suite software. The results obtained prove the possible application of the suggested microscopic technique in the broader diagnostics of abrasive tools.

**Keywords:** Scanning electron microscopy, desktop SEM, abrasive tools, grinding wheel active surface.

### INTRODUCTION

The need to carry out broader and more thorough microscopic research in such fields as material science (composite ceramic materials [1], polymers [2]) and mechanical engineering (precisely machined parts of a machine, elements of measurement machines and research equipment [3], machining tools [4]), forced the producers of SEMs (*Scanning Electron Microscope*) [5] to look for new technical solutions, that meet these expectations. Since the end of the 1980s research has intensified regarding the development of a new generation of SEM's. This research was carried out by the various research laboratories of major global names in the microscope industry, as well as teams of scientists representing the leading universities around the world [6]. This work was mainly concerned with cutting-edge miniaturization of SEM subassemblies, such as miniature low-power electron guns and columns. This issue was more widely discussed by Saini et al. [7,8] and Silver et.

al. [9]. These works resulted in the specification of requirements concerning the architecture, configuration and metrological parameters of the newly developed microscopes, as well as their technical realization in the form of the first prototypical instruments. Due to their state-of-the-art advanced construction and small size, the new instruments were labeled: *benchtop SEM* [10], *portable SEM* [11], *tabletop SEM* [12], *mobile SEM* [13] or *mini SEM* [14]. The first commercial instruments appeared on the market in 2006. One of the more interesting microscopes produced during that period was the Tiny SEM by the Japanese Technex Lab Co., presented a year earlier at the MicroMachine Exhibition Held in Tokyo. Some of its applications were described in [15,16].

More recent desktop SEMs have managed to fill a gap in the instrument's technology, offering a magnification range from  $\sim 150\times$  to  $\sim 60000\times$ , with resolution  $\sim 25\text{-}30$

nm. The ranges of the specified parameters are rather universal (for this class of devices) and make it possible to carry out a number of routine research works without the necessity to purchase expensive specialist devices (e.g. conventional SEMs). Moreover, the desktop SEMs are characterized by many advantages, which include, among others:

- a high quality of acquired image, both in the optical and electron modes (including, considerable depth of field, high contrast),
- a relatively short measurement and operating time (only a few minutes), from the moment the sample is installed in the microscope vacuum chamber to acquisition of first images,
- the small size of the instruments (due to which they can be mounted in rooms with limited space) and their relatively low weight,
- very low energy consumption,
- the possibility of mounting additional extension modules (e.g. for elementary analysis (EDS)),
- user-friendliness (one short course, that lasts less than an hour, is enough to be able to carry out the measurements independently),
- the wide range of applications (automotive, aviation, chemical, materials and metallurgy, microelectronics, energy, microbiology, and pharmaceutical),
- a relatively low price, compared against conventional electron microscopes.

A number of the above mentioned advantages caused a dynamic increase of interest in alternative solutions to conventional SEMs and CLSMs (*Confocal Laser Scanning Microscope*). The main goal of this work is to take a closer look at these solutions as potentially new and effective measurement techniques that may be widely applied in many fields of modern science and technology.

## MATERIALS AND METHODS

The main goal of the experimental tests was to analyze the possibility of utilizing the advanced desktop SEM for the purposes of imaging, measuring and analyzing the abrasive tools active surfaces. The analyses carried out were compared against each other, and other results obtained earlier, using, among other things, the conventional SEM JSM-5500LV by JEOL Ltd., described in the work [4].

### *Sample characteristics and preparation*

Four samples, in the form of miniature grinding wheels with ceramic bond, were selected for the tests. The samples' characteristics are presented in Tab. 1.

**Table 1.** The characteristics of samples used in the experimental tests.

Sample No.	Designation	Surface condition
1.	Grinding wheel 1-35×20×10-99A/F60 K7VDG	Axial breakthrough
2.	Grinding wheel 1-35×10×10- CBN/B126 V	Grinding wheel active surface after internal cylindrical grinding of 100Cr6 steel
3.	Grinding wheel 1-35×20×10-99A/F60 K10VDG	Axial breakthrough
4.	Grinding wheel 1-35×20×10-SG/F80 K7VTO	Axial breakthrough

Before carrying out the measurements and analysis all of the samples had been properly prepared. Each of the samples was placed on a pin stub with 12.7 mm diameter and affixed using conductive graphite based upon isopropanol (isopropyl alcohol), whose trade name is PELCO<sup>®</sup> produced by Ted Pella, Inc. (USA). The conductive graphite consisted of graphite flakes, whose average size were ~1µm (which constituted ~20% of the

volume), and which were connected with cellulose resin and the isopropanol, which performed the role of a dilutant. Graphite after the concentration was placed in a specially designed holder for non-conductive preparations, which was located in the microscope's vacuum chamber.

### *Characteristics of the measurement apparatus*

All observations, measurement and analyses carried out within the framework of the experimental tests were realized by the desktop SEM Phenom G2 Pro produced by Phenom-World (Netherlands). The general view of the microscopic system is shown in Fig. 1.



**Fig. 1.** Advanced desktop SEM Phenom G2 Pro produced by Phenom-World: a) general view of the microscopic system, b) general view and details of standard sample holder for non-conductive preparations with a fixed sample prepared for measurements

Phenom G2 Pro integrated an optical light microscope (with a mag. range from 20× to 120×) and an electron microscope (a mag. range from 80× to 45000×) on one platform. The system was allowed to obtain an image resolution of 25 nm. The electron module included an electron gun, which used cathodes made from cerium boride (CeB6). These long-life cathodes were able to work up to 1000 h. The instrument used a constant accelerating voltage  $U_a = 5\text{kV}$ . The images were

acquired using a color navigation camera equipped with a CCD detector (optical mode) and a highly sensitive backscattered electron detector (electron mode). The image acquisition time was relatively short and was (for the above mentioned modes) respectively: < 5 s and < 30 s. Phenom G2 Pro microscope operated in Linux operations system, using the dedicated Phenom™ Pro Suite computer software (system control, acquisition and simple processing of images) and AnlySIS® by Olympus

(advanced image processing and analysis). The files could have been saved in three typical graphics formats: BMP, TIFF and JPEG, in the following resolutions: 456×456, 684×684, 1024×1024, 2048×2048 pixels. Lawrence *et al.* in their work [17] presented an interesting comparison between the observation – measurement possibilities of Phenom G2 Pro and other SEMs (JEOL JSM 35C and FEI SIRION).

## RESULTS AND DISCUSSION

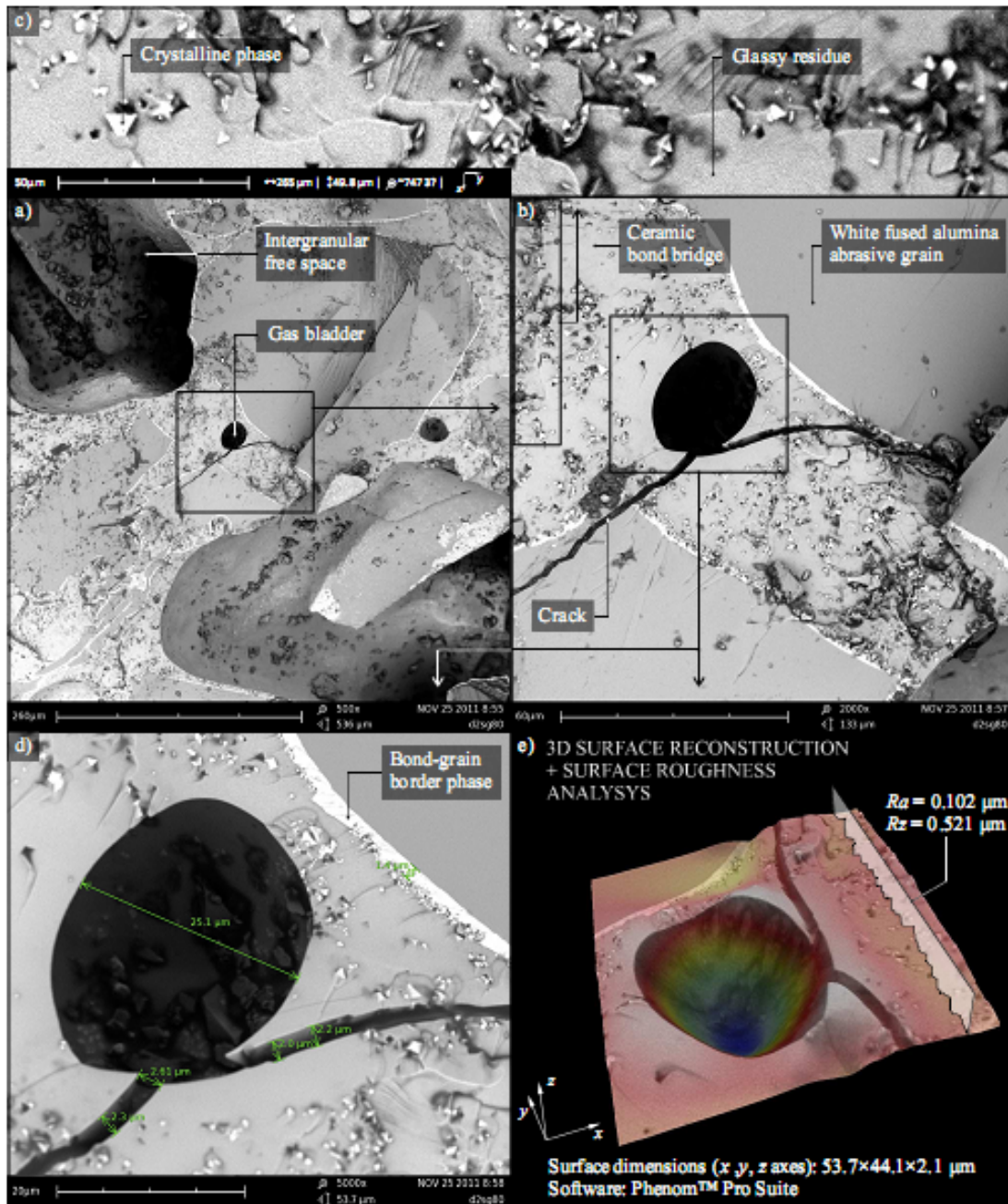
This Section presents select results from the observation and analysis obtained for grinding wheels, whose characteristics were presented in Tab.1. The dedicated software Phenom™ Pro Suite, provided by the microscope producer, was used in all cases. Fig. 2 presents the subsequent phases of observation for the GWAS (Grinding Wheel Active Surface) fragment with the technical designation 1-35×20×10-99A/F60 K7VDG. The input image (Fig. 2a), sized 536×536  $\mu\text{m}$ , acquired in mag. 500×, presents the axial breakthrough of the grinding wheel made from 99A white fused alumina abrasive grains bound with glasscrystalline ceramic bond. The image was selected for analysis due to a number of interesting elements. One of the most interesting of these is the residue of a bladder of gas which was trapped in the ceramic bond bridge during the grinding wheel production process, and the accompanying longitudinal material layer separation propagating through the bond bridge and the abrasive grain. It was created when the sample was being prepared for observation. An AOI (Area of Interest) sized 133×133  $\mu\text{m}$  was extracted from Fig. 2a. This image (Fig. 2b), acquired in mag. 2000×, depicts a more detailed surface structure at the site where the above mentioned elements occurred. Another interesting element is a surface fragment (Fig. 2b, top left) presenting the crystalline phase in the glassy residue of the bond. This fragment, sized 265×49.8  $\mu\text{m}$ , in mag. ~7473×, was extracted and presented in Fig. 2c. In order to analyze the GWAS fragment, which contained local

material structure separation and gas bladder residues, another AOI was extracted from Fig. 2b. Magnified 5000×, the AOI sized 53.7×53.7  $\mu\text{m}$  (Fig. 2d) presents a detailed view of the above mentioned elements. The dimensional assessment of these elements made it possible to estimate, among other things, the bladder diameter (25.1  $\mu\text{m}$ ), the crack width (2.0-2.61  $\mu\text{m}$ ) and the width of the border phase between the bond and the abrasive grain (1.4  $\mu\text{m}$ ). The relatively large magnification revealed the presence of numerous randomly dispersed crystal inclusions of various geometry and size, in the free space created after the gas bladder. The AOI from Fig. 2d also underwent the 3D surface reconstruction procedure and is presented in Fig. 2e. This is a procedure of object visualization in a dimensional system in which the surface element sizes are encoded with indexed colors. 3D surface reconstruction made it possible to estimate the surface dimensions (53.7× 44.1× 2.1  $\mu\text{m}$ ) and selected surface roughness parameters. In this case a surface profile was drawn parallel to the crack visible in the central part. The values of the two surface roughness parameters were determined from the profile: Ra (arithmetic mean deviation of the assessed profile) and Rz (maximum height of the profile within a sampling length). Fig. 3 presents the possibilities of Phenom™ Pro Suite software being able to generate large GWAS fragment panoramas. The large surface fields of the examined objects (sized > 1 mm) can be acquired in the form of a mosaic composed of an n number of properly matched image fragments. The mosaics can be generated in the shape of a square with the same number of rows and columns (e.g. 3×3, 5×5) or a rectangle with a different number of rows and columns (e.g. 5×4, 7×2). Obtaining the resulting image composed of n combined images is connected with carrying out a procedure called image mapping [18] or image stitching [19]. It is one of the standard procedures connected with the acquisition and processing of various

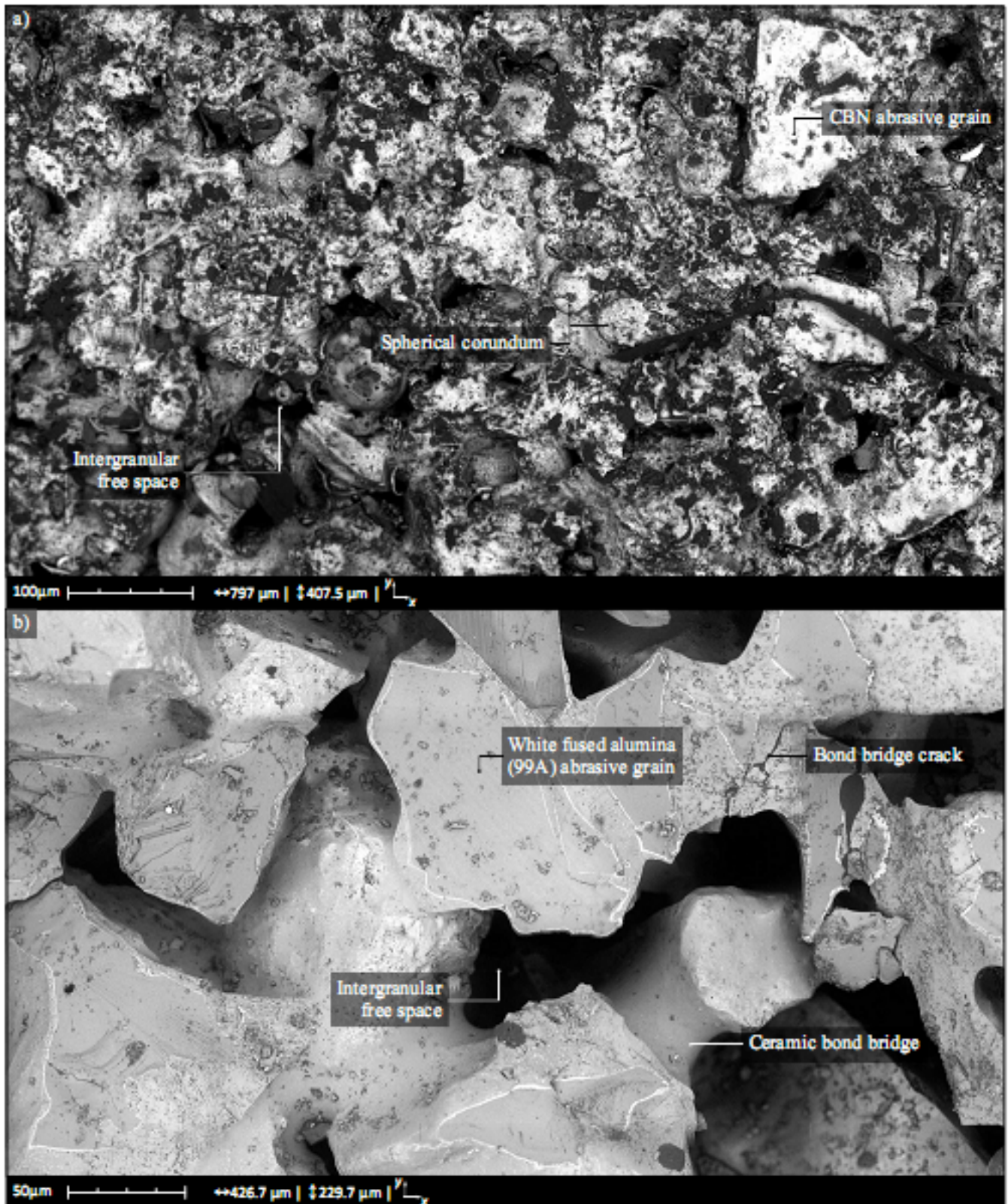
types of measurement data (images, surface maps etc.) used in modern measurement systems.

Fig. 3a presents a panorama of the GWAS fragment with a technical designation 1-35×10×10-CBN/B126V made from CBN (Cubic Boron Nitride) grains bound with ceramic bond. In construction of this grinding wheel a 5% addition of spherical corundum was used, the

breaking of which, when the tool was operating (internal cylindrical grinding of 100Cr6 steel) revealed additional free spaces gathering chips and other grinding products. The input image presented a vast GWAS fragment sized 1.46×1.46 mm (2.14 mm<sup>2</sup>). It was generated through a combination



**Fig. 2.** Collection of select results of experimental tests carried out on the axial breakthrough of the GWAS type 1-35×20×10-99A/F60 K7VDG obtained by using Phenom™ G2 Pro produced by Phenom-World: a) mag. 500×, b) mag. 2000×, c) mag. 7473×, d) mag. 5000×, e) 3D surface reconstruction and surface roughness analysis



**Fig. 3.** Collection of select results of experimental tests carried out on the GWAS type: a) 1-35×10×10- CBN/B126 V, b) 1-35×20×10-99A/F60 K10VDG, obtained by using Phenom™ G2 Pro produced by Phenom-World

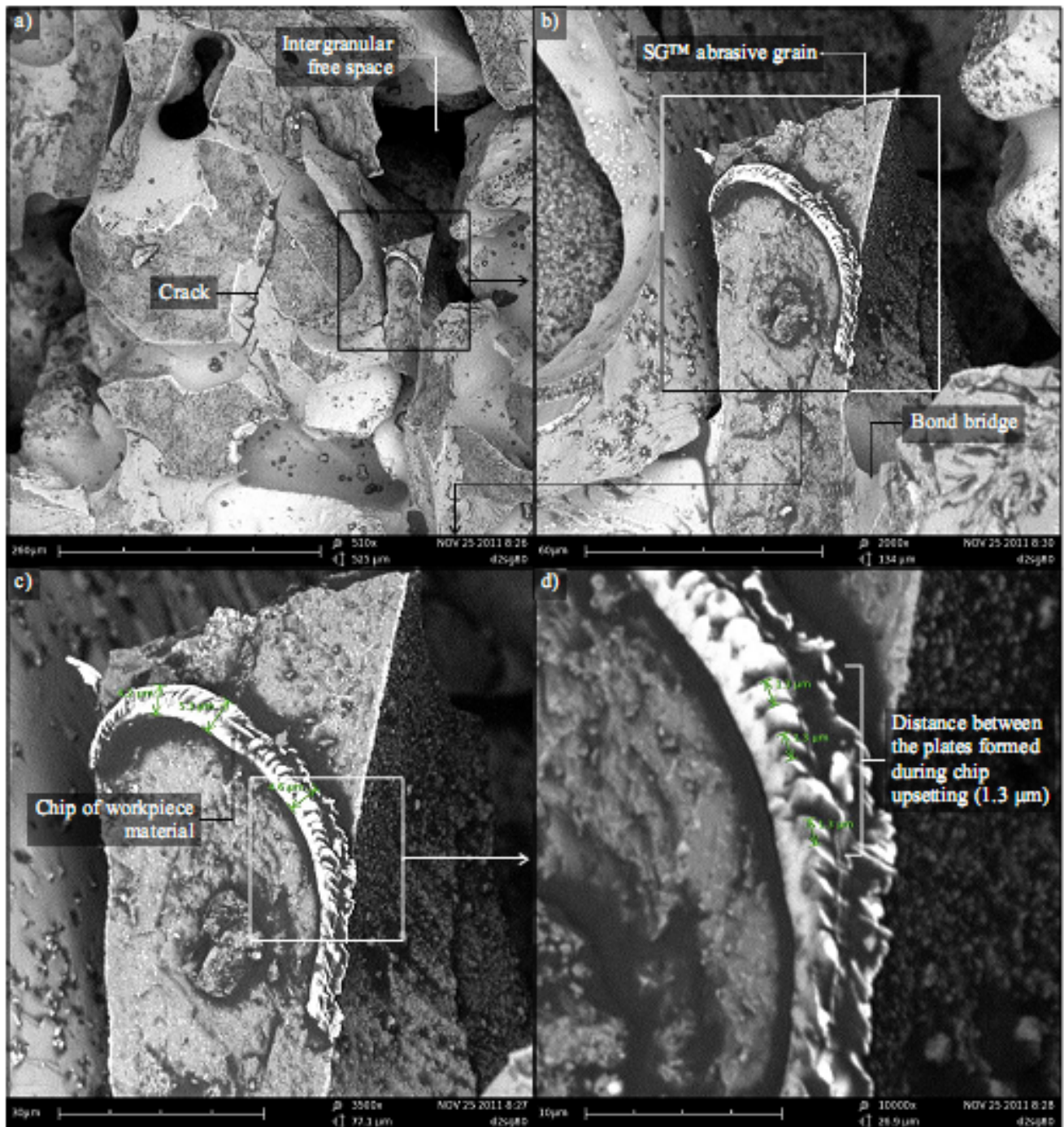


**Fig. 4.** Collection of select results of experimental tests carried out on the axial breakthrough of the GWAS type 1-35×20×10-SG/F80 K7VTO, obtained by using Phenom<sup>TM</sup> G2 Pro produced by Phenom-World: a) mag. 510×, b) mag. 2000×, c) mag. 3500×, d) mag. 10000×.

of 36 (6×6 matrix) single surface images using the automated image mapping procedure. The image acquisition and processing time was 216s. Fig. 3a presents the extracted input image fragment sized 797×407.5 μm. The visual observation of this image makes it possible to analyze the characteristic GWAS elements

such as, among others, abrasive grains and intergranular spaces. Another vast GWAS fragment panorama is presented in Fig. 3b. It is an axial breakthrough of a large-pore grinding wheel with a technical designation 1-35×20×10-99A/F60 K10VDG, characterized by the increasing fractions of intergranular spaces. In this tool

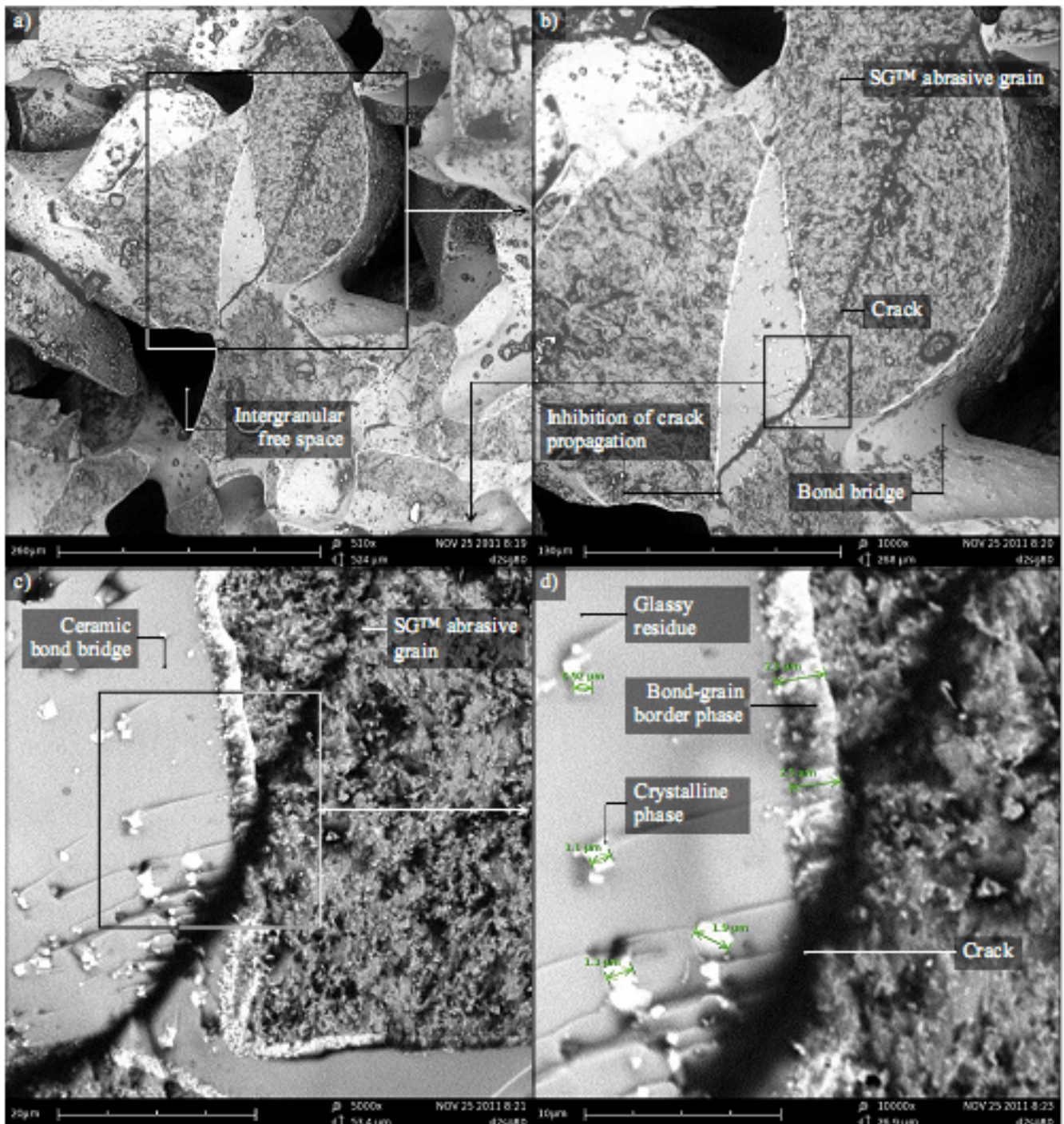


**Fig. 5.** Collection of select results of experimental tests carried out on the axial breakthrough of the GWAS type 1-35×20×10-SG/F80 K7VTO, obtained by using Phenom™ G2 Pro produced by Phenom-World: a) mag. 510×, b) mag. 1000×, c) mag. 5000×, d) mag. 10000×.

the 99A white fused alumina abrasive grains are distanced from each other and connected with bond bridges, creating a very open structure, especially favourable in high-efficiency grinding processes. Just like in the previous case, Fig 3b presents another extracted fragment sized  $426.7 \times 229.7 \mu\text{m}$ , of a larger

input image sized  $1.16 \times 1.24 \text{ mm}$  ( $1.43 \text{ mm}^2$ ). It is a mosaic generated, in this case, through the combination of 25 ( $5 \times 5$  matrix) independent surface images using the automated image mapping procedure. The image acquisition and processing time was 150s. Despite the undeniable advantages of the image results obtained

using the image mapping procedure, certain defects became visible. These were markers, visible in large magnification, which allowed for correct positioning of the connected images. The image processing and combining algorithm used in the procedure left markers that had to be manually removed (retouched) during the possible framing. Nevertheless, the markers would not be noticeable and would not distort the carrying out of observations in a typical visual analysis.

Fig. 4 presents subsequent phases of observation of the axial breakthrough of the grinding wheel made from SG™ microcrystalline sintered corundum grains produced by Norton (Saint-Gobain Group, France), with a technical designation 1-35×20×10-SG/F80K7VTO. An interesting element found on the GWAS fragment was a machined material chip, in this case from steel 100Cr6 with a hardness 62±2 HRC. Fig. 4a is the input image sized 525×525 μm, acquired in mag. 510×, on which the chip adhering to the surface of one of the abrasive grains was identified. The AOI extracted from this image, sized 134×134 μm, acquired in mag. 2000×, made it possible to observe the chip morphology more carefully (including its swelling). To carry out the geometrical measurements of the chip's characteristic elements, another extraction was made, this obtaining an AOI sized 77.1×77.1 μm, acquired in mag. 3500× (Fig. 4c). The lateral dimension of the chip, estimated from a few measurement lengths, ranged from 4.2 to 5.3 μm. The last AOI (Fig. 4d), obtained in mag. 10000×, presents details of the chip morphology. Geometrical measurements were also carried out in this instance. They made it possible to determine values of distances between subsequent plates formed in the process of the chip bulking. The measured distances were the same and were 1.3 μm.

Fig. 5 presents another fragment of the 1-35×20×10SG/F80 K7VTO grinding wheel, which highlights the microstructure of the zone connecting the glasscrystalline bond and the SG™ sintered

microcrystalline corundum grain. As in case of Fig. 4, an AOI was extracted here in subsequent magnifications. An interesting effect observed on the AOI extracted out from the input image, sized 268×268 μm, acquired in mag. 1000× (Fig. 5b), was the method of propagation of the crack which went through the abrasive grain and the bond bridge. The fracture energy was dispersed in the glasscrystalline bond as it encountered the crystals borders. As a consequence the cracking stopped. The subsequent magnifications of the AOI (Fig. 5c-d) allowed for a more detailed analysis of this fragment. Geometrical measurements of the bond crystalline phase crystallites and the width of the border phase, created as a result of contact between the abrasive grain and the bond, were additionally carried out in Fig. 5d.

## CONCLUSIONS

This work, hereby, presents a new dynamically developing variety of electron microscopy, which uses desktop SEMs. One such microscope is the Phenom G2 Pro produced by Phenom-World, operating with the dedicated Phenom™ Pro Suite computer software. The select results of experimental tests presented by the Authors prove the validity of using the presented microscopic technique in diagnostics of abrasive tools. The results obtained confirm the significant potential of the instruments used, mostly due to the high quality and resolution of the images obtained. It may be assumed that a combination of the presented technique with other conventional measurement methods, such as optical profilometry, interferential microscopy, confocal microscopy and scanning electron microscopy, will make it possible to carry out thorough diagnostics of the abrasive tools used in a wide range of machining processes.

## ACKNOWLEDGEMENTS

The Authors wish to thank Mr. Arkadiusz Piersa, M.Sc., B.Sc., and Mr. Bartosz Radkowski, M.Sc., B.Sc., from

Labsoft® (Poland), for carrying out measurements by using the Phenom G2 desktop SEM.

## REFERENCES

- [1] Colorado H.A, Hiel C., Hahn H.Y. (2011) "Processing–Structure–Property Relations of Chemically Bonded Phosphate Ceramic Composites" *Bull. Mater. Sci.* 34(4):785–792.
- [2] Michler G. H. *Electron Microscopy of Polymers*. Springer-Verlag, Berlin, Heidelberg, 2008.
- [3] Li Z.R. *Industrial Applications of Electron Microscopy*. Marcel Dekker, New York, 2003.
- [4] Kaplonek W, Nadolny K. (2013) Assessment of the Grinding Wheel Active Surface Condition using SEM and Image Analysis Techniques. *J. Braz. Soc. Mech. Sci. & Eng.* (in press)
- [5] Reimer L. *Scanning Electron Microscopy: Physics of Image Formation and Microanalysis*. SpringerVerlag, Berlin, Heidelberg, 1998.
- [6] Khursheed A. (1998) Portable Scanning Electron Microscope Designs, *J. Electron. Microsc.* (Tokyo) 47(6):591-602.
- [7] Saini R., Jandric Z., Tsui K., Udeshi T., Tuggle D. (2005) "Manufacturable MEMS Microcolumn" *Microelectron. Eng.* 78-79:62-72.
- [8] Saini R., Jandric Z., Gammell J., Mentink S.A.M., Tuggle D. (2006). Manufacturable MEMS MiniSEMs, *Microelectron. Eng.* 83(4-9):1376-1381.
- [9] Silver C. S., Spallas J. P., Muray L. P. (2007) "Variable Probe Current using a Condenser Lens in a Miniature Electron Beam Column" *Proc. of SPIE* 7378: 737810-1 - 737810-7.
- [10] Šupuk E., Zarrebini A., Reddy J.P., Hughes H., Leane M.M., Tobbyn M.J., Timmins P., Ghadiri M. (2012) "Tribo-Electrification of Active Pharmaceutical Ingredients and Excipients" *Powder Technol.* 217: 427–434.
- [11] Khursheed A. (2001) "Recent Developments in Scanning Electron Microscope Design" *Adv. Imag. Elect. Phys.* 115:197–285.
- [12] Pease R.F.W. (2008) "Significant Advances in Scanning Electron Microscopes (1965–2007)" *Adv. Imag. Elect. Phys.* 150:53–86.
- [13] Inoue M., Suganami M., Hahimoto Y., Iyasu T., Saito H., Moriguchi K., Tanaka T. (2011) "Application of Ionic Liquid Coating Method to Observation of Non-conductive Samples by a Mobile Scanning Electron Microscope for Elementary Science Education" *J. Surf. Anal.* 18(2):105– 109.
- [14] Moona J-I., Leea Y-H., Kima H-J. (2012) "Synthesis and Characterization of Elastomeric Polyester Coatings for Automotive Pre-Coated Metal" *Prog. Org. Coat.* 74(1):125–133.
- [15] Kim, J-W., Taki K., Nagamine S., Ohshima M. (2008) "Preparation of Poly(L-lactic acid) Honeycomb Monolith Structure by Unidirectional Freezing and Freeze-Drying" *Chem. Eng. Sci.* 63(15):3858-3863.
- [16] Kometan R., Nishi S., Warisawa S., Ishihara S. (2011) "Dynamic Characteristics Control of DLC Nano-Resonator Fabricated by Focused-Ion-Beam Chemical Vapor Deposition" *J. Vac. Sci. Technol.* 29(6):06FE03-06FE03-4.
- [17] Lawrence J., Carruthers J., Jiao J. (2007). "Comparison of Materials Characterization Performed by Low Voltage Desktop SEM and Standard High Resolution SEM" *Microsc. Microanal.* 13(Supp. 2):1728-1729.
- [18] Halim F.J., Jin J.S. (2002) "View Synthesis by Image Mapping and Interpolation" *Proceedings of the PanSydney Area Workshop on Visual Information Processing (VIP2001)* (Feng D. D., Jin J., Eades P., Yan H., Eds.), Sydney, Australia, 25-30.
- [19] Kaplonek W., Lukianowicz Cz. (2012) "Coherence Correlation Interferometry In Surface Topography Measurements" [In] *Recent Interferometry*

Applications In Topography And Astronomy (Padron  
I. Ed.). *Intech, Rijeka*, Croatia, 1-26.